The arrojadite–dickinsonite series, $KNa_4Ca(Fe,Mn)_{14}^{2+}Al(OH)_2(PO_4)_{12}$: crystal structure and crystal chemistry

PAUL B. MOORE AND TAKAHARU ARAKI

Department of the Geophysical Sciences
The University of Chicago
Chicago, Illinois 60637

STEFANO MERLINO AND MARCELLO MELLINI

Istituto di Mineralogia
Università di Pisa
56100 Pisa, Italy

AND PIER FRANCESCO ZANAZZI

Istituto di Mineralogia
Università di Perugia
06100 Perugia, Italy

Abstract

The complex crystal structure of the arrojadite–dickinsonite, $KNa_4Ca(Fe,Mn)_{14}^{2+}Al(OH,F)_2(PO_4)_{12}$, series was studied by single-crystal X-ray diffraction techniques. Three compositions were studied and one, dickinsonite from Branchville, Connecticut, is summarized here. The others are arrojadites from the Nancy Mine, North Groton, New Hampshire, and the Nickel Plate Mine, Keystone, South Dakota. Dickinsonite is monoclinic, $a = 24.940(6)$, $b = 10.131(4)$, $c = 16.722(2)$Å, $\beta = 105.60(2)°$, space group $A2/a$, $Z = 4$. $R = 0.078$ for 7740 measured intensities. Of the 49 nonequivalent atoms in the asymmetric unit, fifteen are larger cations, whose coordination polyhedra include six symmetry-independent octahedra, one tetrahedron, one square pyramid, one seven-coordinated polyhedron, two distorted cubes, one non-cubic polyhedron of order eight, two of ten, and one of twelve-coordination.

The arrojadite–dickinsonite structure type is related to that of wyllieite, $Na_2Fe_2^{2+}Al(PO_4)_3$, as seen from a cell with $x_2 = 1/4 - x_1 + z_1$, $y_2 = 1/4 + y_1$, $z_2 = -x_1$, projected down z_2, where (x_1, y_1, z_1) are parameters for the reduced cell used in the refinement. Eliminating disordered Ca in dickinsonite gives the same ratio $\sum(M+X):\sum(P) = 5:3$ as for wyllieite. Average bond distances in dickinsonite are

[4]M(1)–O 2.092,	[5]M(2)–O 2.133,	[6]M(3)–O 2.156,	[6]M(4)–O 2.167,
[6]M(5)–O 2.166,	[6]M(6)–O 2.235,	[5]M(7)–O 2.190,	[6]Al–O 1.884,
[8]X(1)–O 2.516,	[7]X(2)–O 2.515,	[8]X(3)–O 2.574,	[10]X(4)–O 3.012,
[8]X(5)–O 2.928,	[10]X(6)–O 2.940,	[112]X(7)–O 3.080 Å	

The sites M(1), X(1), X(4), X(6), and X(7) are disordered. In addition, one of the six nonequivalent (PO_4) tetrahedra is disordered, with evidence of splitting into a reciprocally coupled P(lx) site, which appears to be directly coupled with the X(6) population.

Introduction

Arrojadite and its isotype dickinsonite are complex primary alkali transition metal phosphates, which have experienced a tumultous investigative history. *Arrojadite* was originally named by Guimarães (1942) for material from the Serra Branca pegmatite,

Parahiba, Brazil; earlier Ziegler (1914) applied the name *soda-triphylite* to an unknown mineral "near-triphylite," originally described by Headden (1891) from the Nickel Plate pegmatite, near Keystone, South Dakota. Quensel (1937) defined this material as *headdenite* in an extensive review of alkali transition metal phosphates from pegmatites. In addition, Mason (1941) reviewed these phases. Lindberg (1950) in an extensive study of arrojadite, hühner-kobelite [= wyllieite group] and graftonite, phases only recently shown to be structurally related, helped clarify the confusion in the literature and pointed out that many so-called arrojadites were in fact a chemically and paragenetically related phase, which she named hühnerkobelite. Moore and Ito (1979) further reviewed these phases, summarized twelve chemical analyses of the arrojadite-dickinsonite family and proposed a formula $X^{1+}Y_3^{1+}M_{14}^{2+}Al(OH,F)(PO_4)_{12}$ where X = large cations (K^+, Ba^{2+}, *etc.*), Y = (Na^{1+},Ca^{2+}) and M = (Fe^{2+}, Mn^{2+} and Mg^{2+}).

The problem was only slightly less confusing for the Mn^{2+}-rich member, dickinsonite. Originally named by Brush and Dana (1878), it persisted as a possible dimorph of fillowite, $Na_2Ca(Mn,Fe)_7^{2+}(PO_4)_6$, and was not recognized as an isotype of arrojadite in Palache *et al.* (1951). Fisher (1965) demonstrated their crystal-chemical relationships through X-ray single-crystal and powder studies, assuming water-free formulae.

About two years ago, P.B.M. and T.A. initiated studies on arrojadite from the Nancy Mine, North Groton, New Hampshire and dickinsonite from the Branchville pegmatite, Connecticut. Almost simultaneously, S.M., M.M., and P.F.Z. completed a structural study of arrojadite from the Nickel Plate pegmatite, South Dakota.

After exchanging notes, we decided to combine the three studies in one paper. Krutik *et al.* (1979) announced their crystal structure analysis of arrojadite (Nickel Plate); although we agree with these authors on the broad structural features, four additional larger cation sites and one PO_4 site have been discovered, all of them only partly occupied and consequently disordered.

We feel that these minerals are important, relatively high temperature phases (~800°C), which are practically confined to granitic pegmatites, and which, due to their olive- to grass-green appearance, are often misidentified as the more prevalent triphylite–lithiophilite. Since practically nothing is known about their thermochemical stabilities other than their paragenetic appearance, we also suspect that they may be key phases in unravelling pegmatite genesis and crystallization sequences.

Experimental

Experimental details on three specimens of arrojadite–dickinsonite are summarized in Table 1: abbreviations are NM for Nancy Mine, North Groton, New Hampshire arrojadite (analysis No. 7 in Moore and Ito, 1979); NP for Nickel Plate, Keystone, South Dakota arrojadite (Lindberg, 1950; Merlino *et al.*, 1981) and BR for Branchville, Connecticut dickinsonite. The NM and BR data were collected by Moore and Araki, and the NP data by Merlino, Mellini and Zanazzi. The NM sample was from a large crystal section kindly donated by Mr. Clayton Ford, and the BR material corresponds to a Brush and Dana specimen, Yale University No. 3090. We also thank Mr. Willard L. Roberts who donated to Moore and Araki a large specimen from the Nickel Plate Mine.

Crystal cell parameters were obtained by least-squares fits of data obtained from the mounted single-crystals just prior to intensity collection. Reference reflections were monitored to assess machine stability. Although the studies were done by two groups independently, we followed almost identical procedures. First, a solution from the Patterson synthesis was attempted, but the pronounced homometricity of the metal interatomic vectors failed to yield a reasonable model. Direct methods were then applied utilizing the program MULTAN (Main *et al.*, 1977) and a sufficient number of heavy atoms was located to phase about 2000 of the more prominent F_0. Successive Fourier and difference syntheses admitted location of all atoms in the asymmetric unit. For structure refinement neutral atom scattering factors were used for NP; but P^0, O^{1-} and the charges of the larger cations indicated in Table 7 were used for NM and BR. The selection of the appropriate scattering curves for the sites was guided by (1) height of the peaks in the final electron density map, (2) thermal vibration ellipsoids, (3) coordination geometry and mean bond distances, and finally, (4) chemical analyses, which are reproduced in Table 8 for the appropriate samples. Scattering curves were obtained from Ibers and Hamilton (1974). For NM and BR anomalous dispersion corrections based on angular dependence were applied to all atoms following Cromer and Mann (1968).

Toward the end of the refinement, the samples showed residual electron density requiring a splitting of P(1) into the P(1x) position as well, whose density complemented the deficit at P(1). In addition, an-

Table 1. Experimental details of arrojadite–dickinsonite

(A) Crystal Cell Data

	NM	NP	BR
a, Å	24.692(4)	24.730(5)	24.940(6)
b, Å	10.031(2)	10.057(3)	10.131(4)
c, Å	16.453(2)	16.526(4)	16.722(2)
β, deg	105.72(9)	105.78(3)	105.60(2)
Space group	A2/a	A2/a	A2/a
Z	4	4	4
Formula (ideal)†	$KNa_4Ca(Fe,Mn)^{2+}_{14}Al(OH,F)_2(PO_4)_{12}$		
ρ(calcd), g cm^{-3}*	3.586	3.538	3.426
Specific gravity*	3.527	3.553	3.41
μ, cm^{-1}	55.0	54.5	52.3

(B) Intensity Measurements

Crystal size, mm	$0.20(\|\|a) \times 0.40(\|\|b) \times 0.24(\|\|c)$	sphere, 0.6 mm diameter	$0.14(\|\|a) \times 0.27(\|\|b) \times 0.29(\|\|c)$
Crystal orientation	$\phi\|\|b$, PICKER FACS-1	PHILIPS PW 1100	$\phi\|\|b$, PICKER FACS-1
Max$(\sin\theta)/\lambda$	0.75	0.79	0.75
Scan speed, deg per min	1.0	2.4	1.0
Base scan width	1.6	1.4	1.7
Background counts	Stationary, 20 s at beginning and end of scan		
Radiation	MoKα	MoKα	MoKα
Independent F_0	6905	6910	7158
Measured intensities	7116	8069	7740

(C) Refinement of the Structure

R	0.075	0.063	0.078
Scale factor	1.094(3)	---	2.168(7)
Coefficient of extinction	$1.8(2) \times 10^{-7}$	---	$5(1) \times 10^{-8}$

*The specific gravity of BR is from Wolfe (1941), NP from Lindberg (1950) and NM from this study. Calculated densities use the formulae of Table VII in Moore and Ito (1979) except that the calculation was normalized to 200 anions in the unit cell.

†Assumes 84 cations in the cell and no solution between Ca, Na, and (Fe,Mn).

other electron density, that of X(6), seemed to be coupled to that of P(lx). Finally, a partly occupied large cation site of order 12 was found toward the final stages of refinement and difference synthesis; it was labelled X(7).

Final atomic coordinate parameters for NM, NP, and BR appear in Table 2, anisotropic thermal vibration parameters for NM and BR in Table 3, ellipsoids of vibration for NM and BR in Table 4, structure factors in Table 5[1] and bond distances and

[1] To obtain a copy of Table 3, order Document AM-81-168; Table 4, AM-81-169; and Table 5, order Document AM-81-170 from the Business Office, Mineralogical Society of America, 2000 Florida Avenue, N.W., Washington, D.C. 20009. Please remit $1.00 in advance for each microfiche. These tables include NM and BR; NP was earlier deposited by Merlino et al. (1981).

angles in Table 6. The order of increasing O—O′ distances in the individual polyhedra with respect to polyhedral type is summarized in Table 6a.

In many of these tables, it was not necessary to repeat what was already published. In particular, the Merlino et al. (1981) study covers some of these details for NP. The emphasis was placed on a comparison between two members of a series, the Fe^{2+}-rich member arrojadite from NM and the Mn^{2+}-rich dickinsonite from BR.

Final R-indices for the three studies appear in Table 1, where

$$R = \frac{\sum ||F_o| - |F_c||}{\sum |F_o|} .$$

The final cycles minimized $\sum_w ||F_o| - |F_c||^2$ where w = $\sigma^{-2}(F)$.

The calculated densities in Table 1 are in fair agreement with measured densities when a total of 200 anions in the unit cell is used. The density calculation proceeded from the cell parameters in this table and the chemical analyses in Table 8. The differences may reflect some component or components not having been discovered in the chemical and/or structural analyses, since arrojadites usually show a large number of components present. Disorder over several larger cation sites would also contribute to this effect since high correlations exist among the scattering curves used and the site population refine-ment. In addition, complex solid solution may involve at least one component whose scattering curve was not employed. Indeed, the severely anisotropic thermal vibration ellipsoids in Table 4 for X(1), X(2), X(4) and X(5) suggest that these large "wastebasket" sites would require yet another technique if their populations and species were to be more precisely assessed. Arrojadite–dickinsonite is probably the most complicated of all mineral structures, even when studied by modern crystal structure analytical techniques.
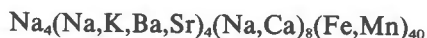
The tables also suggest that the study of Krutik *et*

Table 2. Arrojadite–dickinsonite series atomic coordinates[†]

	NM			NP			BR		
	x	y	z	x	y	z	x	y	z
A1	0	½	0	0	½	0	0	½	0
M(1)	0.47321(6)	0.89531(14)	0.22048(8)	0.4738(1)	0.8957(2)	0.2202(1)	0.47856(7)	0.88682(18)	0.22519(10)
M(2)	0.26656(3)	0.00954(6)	0.21173(4)	0.2674(1)	0.0078(1)	0.2123(1)	0.26879(4)	0.00654(8)	0.21154(6)
M(3)	0.14023(4)	0.01559(9)	0.10524(6)	0.1394(1)	0.0142(1)	0.1066(1)	0.13944(3)	0.01293(8)	0.10620(5)
M(4)	0.40367(3)	0.25041(7)	0.02298(4)	0.4036(1)	0.2496(1)	0.0222(1)	0.40442(3)	0.24825(8)	0.02195(5)
M(5)	0.39990(2)	0.74383(6)	0.03394(4)	0.4004(1)	0.7434(1)	0.0334(1)	0.40102(3)	0.74524(8)	0.03375(4)
M(6)	0.35132(3)	0.70124(7)	0.20352(4)	0.3517(1)	0.6992(1)	0.2044(1)	0.35182(3)	0.69839(8)	0.20674(5)
M(7)	0.34199(3)	0.29518(8)	0.21822(5)	0.3432(1)	0.2945(1)	0.2193(1)	0.34356(4)	0.29531(9)	0.22190(5)
X(1)	0.48587(9)	0.22363(22)	0.23404(14)	0.4848(1)	0.2223(3)	0.2322(2)	0.48542(9)	0.22242(22)	0.23362(13)
X(2)	0.11986(11)	0.51637(25)	0.13523(29)	0.1202(2)	0.5150(4)	0.1289(4)	0.12070(12)	0.51223(27)	0.12679(25)
X(3)	0	0	0	0	0	0	0	0	0
X(4)	¼	0.1248(11)	0	½	0.1460(18)	0	¼	0.1600(17)	0
X(5)	¼	0.5090(2)	0	½	0.5043(5)	0	¼	0.4960(4)	0
X(6)	0.4560(6)	0.9448(16)	0.2037(8)	0.4567(4)	0.9417(9)	0.2077(6)	0.45639(33)	0.93751(82)	0.21059(45)
X(7)	¼	0.9192(27)	0	¼	0.9192(42)	0	¼	0.9079(25)	0
P(1)	0.36662(6)	0.01006(13)	0.11457(9)	0.3662(1)	0.0085(3)	0.1130(2)	0.3693(1)	0.0090(2)	0.1168(2)
O(1)	0.3677(1)	0.0625(3)	0.0258(2)	0.3675(3)	0.0614(5)	0.0250(3)	0.3680(2)	0.0624(4)	0.0281(2)
O(2)	0.3633(1)	-0.1412(3)	0.1122(2)	0.3635(4)	-0.1416(5)	0.1120(4)	0.3643(2)	-0.1396(4)	0.1139(2)
O(3)	0.3179(5)	0.0734(12)	0.1382(7)	0.3220(4)	0.0770(7)	0.1426(5)	0.3235(3)	0.0762(6)	0.1455(4)
O(4)	0.4220(2)	0.0469(5)	0.1821(3)	0.4222(5)	0.0462(10)	0.1807(6)	0.4246(3)	0.0410(7)	0.1799(4)
P(1x)	0.3344(2)	0.9972(5)	0.0803(3)	0.3354(2)	0.9948(5)	0.0799(3)	0.3388(2)	0.9987(4)	0.0847(3)
O(3x)	0.2718(8)	0.9540(20)	0.0224(12)	0.2720(9)	0.9678(45)	0.0234(14)	0.2713(11)	0.9691(26)	0.0277(16)
O(4x)	0.3231(9)	0.0860(26)	0.1479(13)		Equal to O(4)		0.3473(11)	0.0797(29)	0.1642(17)
P(2)	0.42435(4)	0.46788(11)	0.13165(7)	0.4246(1)	0.4670(1)	0.1303(1)	0.42283(5)	0.46775(13)	0.12855(8)
O(5)	0.4456(1)	0.4443(3)	0.0519(2)	0.4450(2)	0.4448(5)	0.0501(3)	0.4438(2)	0.4455(4)	0.0496(2)
O(6)	0.3909(1)	0.5970(3)	0.1207(2)	0.3924(3)	0.5879(5)	0.1213(3)	0.3907(2)	0.5974(4)	0.1190(2)
O(7)	0.3872(1)	0.3430(3)	0.1317(2)	0.3871(3)	0.3445(5)	0.1301(4)	0.3854(2)	0.3460(4)	0.1281(2)
O(8)	0.4725(2)	0.4678(4)	0.2131(2)	0.4733(3)	0.4637(7)	0.2103(4)	0.4702(2)	0.4652(5)	0.2086(2)
P(3)	0.03946(4)	0.25200(10)	0.12684(6)	0.0385(1)	0.2518(2)	0.1259(1)	0.03808(5)	0.24996(13)	0.12487(8)
O(9)	0.0752(1)	0.1662(3)	0.0843(2)	0.0751(2)	0.1664(5)	0.0842(3)	0.0733(2)	0.1649(4)	0.0818(2)
O(10)	0.0367(1)	0.3958(3)	0.0950(2)	0.0360(2)	0.3951(5)	0.0941(3)	0.0370(2)	0.3924(4)	0.0944(2)
O(11)	-0.0199(1)	0.1897(3)	0.1101(2)	-0.0206(2)	0.1891(6)	0.1078(4)	-0.0208(2)	0.1911(4)	0.1070(2)
O(12)	0.0644(1)	0.2542(3)	0.2238(2)	0.0623(2)	0.2533(6)	0.2224(3)	0.0622(2)	0.2476(4)	0.2206(2)
P(4)	0.04849(4)	0.76821(10)	0.10200(7)	0.0474(1)	0.7673(2)	0.1023(1)	0.04757(5)	0.76632(13)	0.10221(8)
O(13)	0.0489(1)	0.6431(3)	0.0458(2)	0.0482(2)	0.6428(5)	0.0467(3)	0.0485(2)	0.6431(4)	0.0467(2)
O(14)	0.0803(1)	0.8734(3)	0.0636(2)	0.0794(2)	0.8719(5)	0.0652(3)	0.0789(2)	0.8710(4)	0.0646(2)
O(15)	-0.0114(1)	0.8142(3)	0.0967(2)	-0.0126(2)	-0.8139(6)	0.0961(4)	-0.0114(2)	0.8122(4)	0.0976(3)
O(16)	0.0793(1)	0.7371(4)	0.1939(2)	0.0770(3)	0.7357(6)	0.1939(4)	0.0773(2)	0.7359(4)	0.1929(2)
P(5)	0.21262(4)	0.72485(11)	0.12932(7)	0.2115(1)	0.7241(2)	0.1304(1)	0.21185(5)	0.72319(13)	0.12967(8)
O(17)	0.1712(1)	0.6753(4)	0.0486(2)	0.1703(3)	0.6785(6)	0.0484(4)	0.1713(2)	0.6816(4)	0.0473(2)
O(18)	0.2709(1)	0.6765(4)	0.1296(2)	0.2703(2)	0.6781(6)	0.1315(4)	0.2705(2)	0.6807(4)	0.1302(3)
O(19)	0.2105(2)	0.8783(4)	0.1348(3)	0.2088(3)	0.8773(6)	0.1395(4)	0.2091(2)	0.8742(4)	0.1403(3)
O(20)	0.1952(1)	0.6648(4)	0.2057(2)	0.1938(3)	0.6604(6)	0.2044(4)	0.1936(2)	0.6563(4)	0.2018(2)
P(6)	0.20536(5)	0.30030(11)	0.14028(8)	0.2045(1)	0.2972(2)	0.1425(1)	0.20441(5)	0.29526(13)	0.14445(8)
O(21)	0.1646(1)	0.3456(4)	0.0562(2)	0.1653(2)	0.3402(6)	0.0583(4)	0.1665(2)	0.3376(4)	0.0602(3)
O(22)	0.2644(2)	0.3551(4)	0.1456(4)	0.2632(3)	0.3509(8)	0.1516(6)	0.2629(2)	0.3503(5)	0.1545(3)
O(23)	0.2055(1)	0.1470(3)	0.1443(3)	0.2052(2)	0.1447(5)	0.1489(4)	0.2058(2)	0.1438(4)	0.1494(3)
O(24)	0.1847(2)	0.3561(4)	0.2151(3)	0.1824(3)	0.3541(6)	0.2156(4)	0.1813(2)	0.3499(4)	0.2155(2)
F	0.1395(2)	0.0035(3)	0.2301(2)	0.1383(3)	0.0013(5)	0.2315(3)	0.1354(2)	0.0009(4)	0.2309(3)

[†]Estimated standard errors refer to the last digit.

al. (1979) does not tell the complete story. The latter authors admit that their unit cell contents display a deficit of Na^+ ions and propose the formula:

$$Na_4(Na,K,Ba,Sr)_4(Na,Ca)_8(Fe,Mn)_{40}$$

$$Al_4(Li,Mg,Ca,Al,Fe,Mn)_{16}$$

$$[PO_4]_{32}[PO_3(O,F,OH)]_{16}(OH)_8,$$

which yields a total of 76 larger cations in the cell. In Table 7[2], their nomenclature is listed and we note that they did not report disordered X(1), X(4), X(6) and X(7). In addition, we found disordered P(1) in our refined structures. Moore and Ito (1979) proposed 83.43 larger cations in the cell, the same number listed by Merlino et al. (1981), both conclusions being based on studies of the Nickel Plate material.

Description of the structure

Although we utilized the reduced cell for structure refinement, a better structural description admits a projection down the [101] direction or its inverse. This projection, based on the Nancy Mine arrojadite, has $a' = 16.45$, $b = 10.03$, $c' = 25.70$Å, $\beta' = 112.33°$, space group $C2/c$, with transformation from the old reduced coordinate system (x_1, y_1, z_1) to the new (x_2, y_2, z_2): $x_2 = 1/4 - x_1 + z_1$, $y_2 = 1/4 + y_1$, $z_2 = -x_1$. Projecting the cations only (X, M and P) down [001] in this new coordinate system gives the representation in Figure 1. Circular contours are drawn around the six discrete cationic rods, which are referred to by Roman numerals. If their circular contours are shrunk to poles or lines, Figure 2 results with disordered P(1x), X(1), X(6) and X(7) left out. This figure is an idealization of Figure 1. The net, neither regular nor semiregular, consists of two kinds of polygons, the regular hexagon and the regular rhombus (which when bisected is made up of two equilateral triangles). Nodes of this net consist of two kinds when the triangles are substituted in place of rhombuses: $\{6 \cdot 3 \cdot 6 \cdot 3\}$ and $\{6 \cdot 6 \cdot 3 \cdot 3\}$. All cations can be identified with regions of this net. The distinct rods and their occupancies can be summarized as follows:

Rod I	center of hexagon	M(2),M(3),Al,X(2), X(3)
Rod II	rhombus center	disordered X(1), $\square$
Rod III	$\{6 \cdot 3 \cdot 6 \cdot 3\}$ node	M(1),X(4),X(5),X(6), X(7),P(1),P(2)

[2] To obtain copy of Table 7, order Document AM-81-171. See footnote one for complete details.

Rod IV	$\{6 \cdot 6 \cdot 3 \cdot 3\}$ node	M(5),M(6),P(3),P(5)
Rod V	$\{6 \cdot 6 \cdot 3 \cdot 3\}$ node	M(4),M(7),P(4),P(6)
Rod VI	rhombus center	$\square$ (at origin)

We shall see that X(4), X(6), X(7) and P(1) involve rather complex disorder and coupled relationships. In this way all cations are accounted for in arrojadite's structure type, bearing in mind that X(1), X(6) and X(7) can only be at most half-occupied for steric reasons and that X(4) evidently can take on a range of populations.

Wyllieite (Moore and Molin-Case, 1974) shares with arrojadite the same kind of net, but its ordering scheme is much simpler, as is its unit cell. Its projection (Fig. 3) has been discussed previously (Moore, 1981). A correspondence between the two cells reveals $a\sin\beta$ (wyl) $\sim b$ (arr); b (wyl) $\sim a\sin\beta$ (arr); $4c\sin\beta$ (wyl) $\sim c\sin\beta$ (arr) or expressed as cell translations for wyllieite and arrojadite, respectively, $10.80 \sim 10.03$; $12.38 \sim 15.21$; $23.11 \sim 23.78$ or the ratios with wyllieite as the divisor 0.929 : 1.229 : 1.029. Aside from chemical differences, the most pronounced difference is substantial stretching in the [100] direction in arrojadite, which is the direction toward opposing $\{6 \cdot 3 \cdot 6 \cdot 3\}$ nodes through the chain of corner-linked hexagons. This is particularly noticeable in Figure 1 where the eight cations in rod I are arrayed along the [100] direction. Disorder of some of the cations, discussed subsequently, also contributes to this effect. In particular X(1), which occupies the rhombus of rod II, "stretches" the rhombus along the [100] direction.

Fifteen distinct larger cations and six distinct PO_4 tetrahedra occur in the asymmetric unit of the structure. Seven of the former cations are labelled M and correspond to populations where transition metal cations predominate. The cations M(3), M(4), M(5), and M(6) are associated with distorted octahedra, M(1) a distorted tetrahedron, M(2) a distorted square pyramid, and M(7) either a square pyramid or an octahedron when disordered and partly occupied with O(4x) included as a coordinating anion. The Al atom resides in a distorted octahedral site at an inversion center and is clearly essential in the crystal structure. The remaining independent large cation sites are labelled X. The sites X(2), X(3), and X(6) are predominately occupied by Na^{1+}; X(1) is a half-occupied Ca^{2+} site and X(4), X(5) and X(7) are large sites occupied principally by K^+ or Na^+. The X(1) site of order 8 corresponds to polyhedron No. 44 of order 8 and maximal point symmetry C_2, following
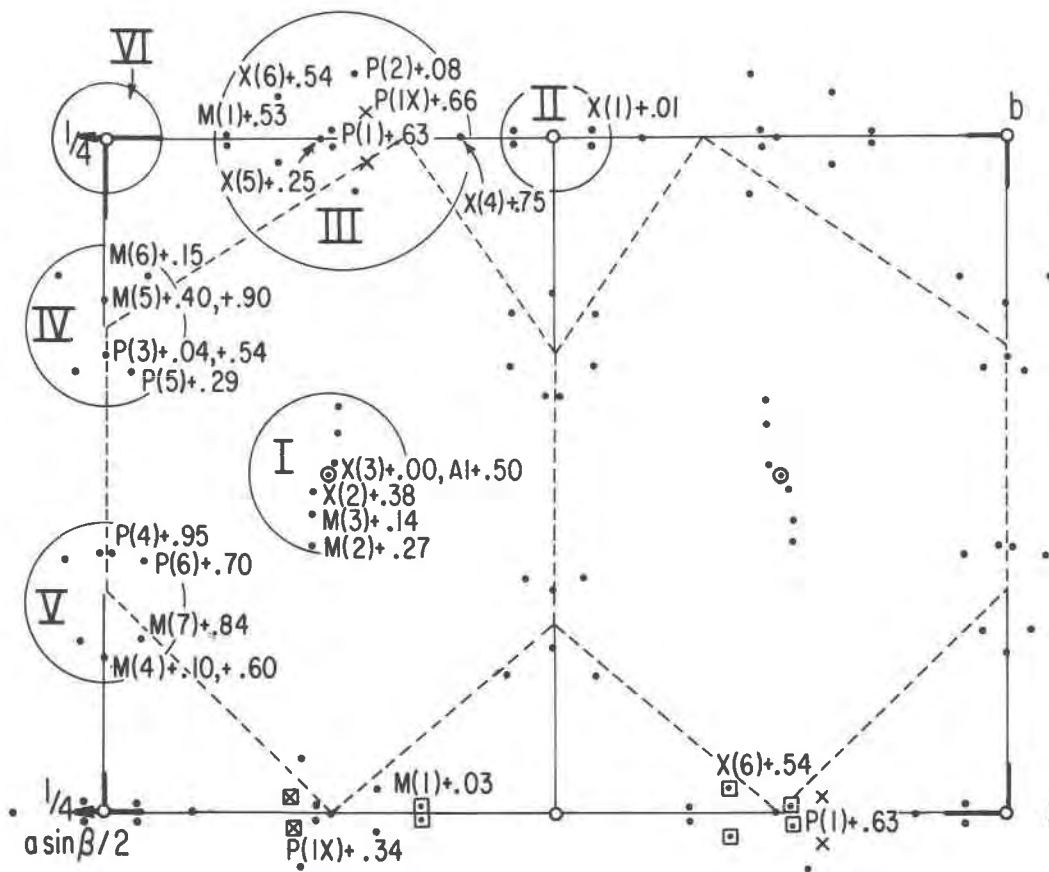
Fig. 1. Plan of the arrojadite (NM) structure down [001] of the transformed cell (see text). The circles envelop the larger cations in the asymmetric unit and the Roman numerals refer to the nonequivalent rods in the structure. Inversion centers are shown as open circles and 2-fold rotors as arrows. Heights are given as fractional coordinates along z. Cations which display a coupled relationship are shown as squares at $x = 1/2$. The P(1x) is labelled as crosses. The $\{6 \cdot 3 \cdot 6 \cdot 3\}$ and $\{6 \cdot 6 \cdot 3 \cdot 3\}$ net is dashed.

the nomenclature of Britton and Dunitz (1973); X(2) is a distorted cube (Table 6) if the long X(2)–O(12) 3.46Å distance is included. Neglect of this distance gives polyhedron No. 29 of order 7 and maximal point symmetry C_{3v}, consisting of three squares and four triangles. The X(3) and X(5) sites are in distorted cubes; X(4) is in a complex polyhedron of order ten and consists of six triangles, three squares and a hexagon with maximal point symmetry C_{2v}. The disordered site X(6) resides in a ten-coordinated site with X(6)–O ranging from 2.11 to 3.60Å in NM arrojadite. The first four distances are below 2.53Å, the remaining six greater than 3.22Å. Disordered site X(7) is coupled with X(4), and can be fully occupied only if X(4) is empty. In all three crystals which we studied X(7) is only weakly occupied and corresponds to a distorted cuboctahedron of order 12.

Arrojadite's crystal chemistry is further complicated by disorder due to steric hindrance at eleven sites: M(1), X(1), X(4), X(6), X(7); and P(1), O(3), O(4) and P(1x), O(3x), O(4x). The sites X(6), P(1) and P(1x) are coupled. If P(1) is vacant, P(1x) and X(6) are occupied. If a portion of X(6) is occupied, a corresponding portion of M(1) must be absent due to steric hindrance. X(1) is close to an inversion center such that the X(1)–X(1)[(6)] separations of 0.9–1.0Å occur in these structures and the site is half-occupied. This is the only site which does not occur at a nodal point or in a hexagon's center but at the center of a rhombus and corresponds to label II in Figure 2. The remaining site, X(4) (Fig. 1), is sufficiently removed from other cations to suggest that it could remain fully occupied without experiencing violent cation–cation repulsion effects. It is coupled to X(7), with X(4)–X(7) = 2.28Å for NP arrojadite, which has 0.17 site population with Na^{+} (Table 7). The other most
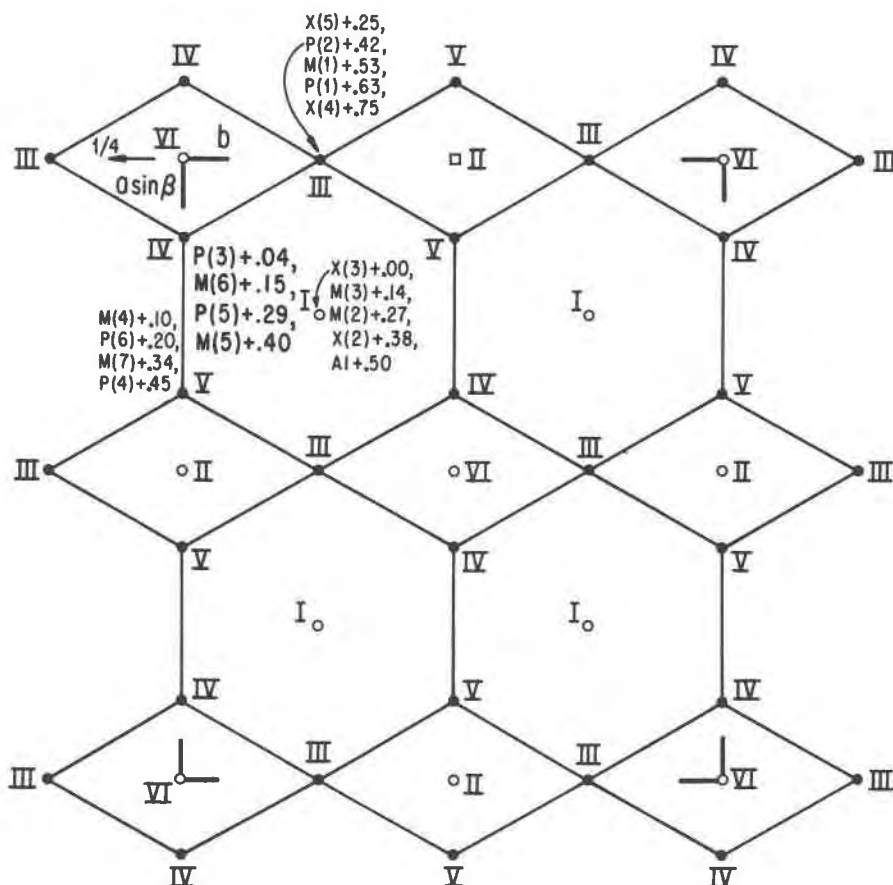
Fig. 2. Idealization of Figure 1 based on the $\{6 \cdot 3 \cdot 6 \cdot 3\}$ and $\{6 \cdot 6 \cdot 3 \cdot 3\}$ net constructed of rhombuses (two equilateral triangles with a common edge) and hexagons. The disordered cations P(1x), X(1), X(6) and X(7) have been left out. Note a c-glide plane occurs at $b = 0$ and a 2-fold rotor parallel to b at $c = 1/4$. Open circles refer to inversion centers at $z = 0$, $1/2$.

likely close contact is with P(1x) with an X(4)–P(1x) separation of about 2.5–2.8Å, suggesting that X(4) populations are also reciprocally related to P(1x) populations. But Table 7 suggests that this coupling is not so strong as the direct relationship between P(1x) and X(6) which appear to be truly coupled in a cooperative manner. Figure 1 features a possible distribution of populated and unpopulated cations along the line at $x = 1/2$.

The same argument was used for wyllieite's crystal chemistry by Moore and Molin-Case (1974). In that structure, the size of the large cations was X(2) > X(1a) > X(1b) with average X–O distances 2.64, 2.53 and 2.21Å respectively. In that structure, the site distributions X(2) = 2.78 Na^{1+} + 1.22□, where □ represents a vacancy; and X(1a) = 1.82 Na^{1+} + 0.18□. By analogy, we propose a sequence of omission X(7) > X(4) > X(5) > X(3) with average X–O distances 3.08 (for NP), 2.98, 2.82 and 2.56Å for NM arrojadite.

Summarizing, the following conditions appear to hold for arrojadite:

a) If the X(6) population is (x), the M(1) population is $(1 - x)$;
b) X(1) is half-populated;
c) The X(4) population at most equals the P(1) population. X(7) is reciprocally related to X(4).
d) The X(6) population equals the P(1x) population;
e) If the P(1x) population is (y), the P(1) population is $(1 - y)$.

This is easily seen in the distances between cations. They are M(1)–X(6) = 0.66, X(1)–X(1)$^{(6)}$ = 0.92, X(4)–P(1x) = 2.50, X(4)–X(7) = 2.28 (for NP), X(6)–P(1) = 2.39 and P(1)–P(1x) = 0.85Å for NM arrojadite.

Taking the aforementioned conditions into account, the following sites can at most be half-occupied: X(1) and X(6). With P(1x) completely empty, X(4) could be fully occupied and X(7) would be empty. Taken together the maximal site occupancy would be 4X(1)(+4□) + 8X(2) + 4X(3) + 4X(4) + 4X(5) + 4X(6)(+4□) + 0X(7) + 4M(1)(+4□) +
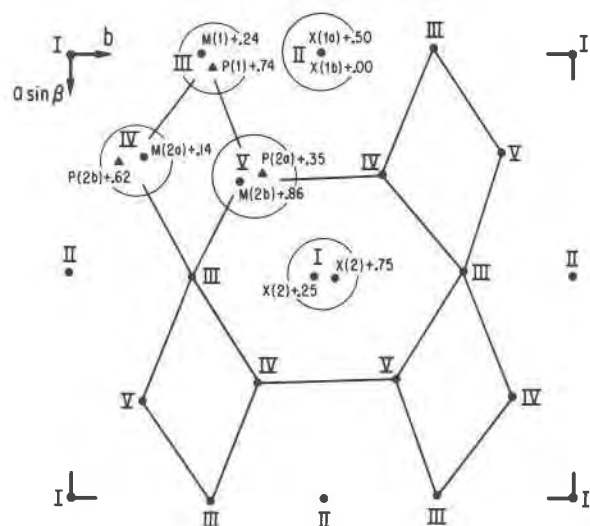
Fig. 3. The cations in the wyllieite structure (Moore and Molin-Case, 1974) with a portion of the {6 · 3 · 6 · 3} and {6 · 6 · 3 · 3} net drawn in. The structure is projected down [001] and preserves the axes and coordinates of the original study.

8M(2) + 8M(3) + 8M(4) + 8M(5) + 8M(6) + 8M(7) + 4Al or 84 larger cations per 48 P^{5+} atoms. Omitting partly occupied X(6) leads to $\sum(X+M):\sum P = 80:48$ in the cell or 5:3, exactly the ratio for the related crystal structure of wyllieite and discussed in considerable detail (Moore, 1981). Wyllieite is ideally $Na_2Fe_2^{2+}Al(PO_4)_3$. The arrojadite end member would ideally be $KNa_4CaFe_{14}^{2+}Al(F,OH)_2(PO_4)_{12}$, but in such a complex structure with a limited but variegated range of vacancies and with some deficit of PO_4 occupancies as seen in chemical analyses, no precise formula can be expressed. Solid solution of the type found in fillowite (Araki and Moore, 1981) also exists and involves (K,Na), (Na,Ca) and (Na,Ca,Fe). In the "ideal" formula occupied X(5) identifies with K^{1+}; X(2), X(3) and X(6) with Na^{1+}; X(1) with Ca^{2+}; and M(1) through M(7) with Fe^{2+}. Further on, we discuss the role of Li^{1+} in the structure. This small alkali cation almost certainly occurs at the unusual M(1) tetrahedral site and may be important for the structure's stability. Evidence from the structure study suggests that the X(4) site may accommodate extensive Na^{1+} instead of K^{1+}. Much like the feldspar structures the large X(4) site may exhibit smaller cations which display pronounced thermal vibration or local positional disorder which is concealed in the thermal vibration parameters, rather being in this case residency parameters. The X(7) site unfortunately is so weakly populated that refinement of site population and thermal vibration do not admit discussion on the kind of ionic species present.

Selecting a particular ordering scheme, arrojadite's structure can be described, as was fillowite's, as a rod packing. Following Figure 2, each rod can be described as a sequence of cations along z. Eight cations constitute the repeat, so that $c'/8 = 25.70/8 = 3.21Å$ which would correspond to $c/2 = 3.18Å$ in
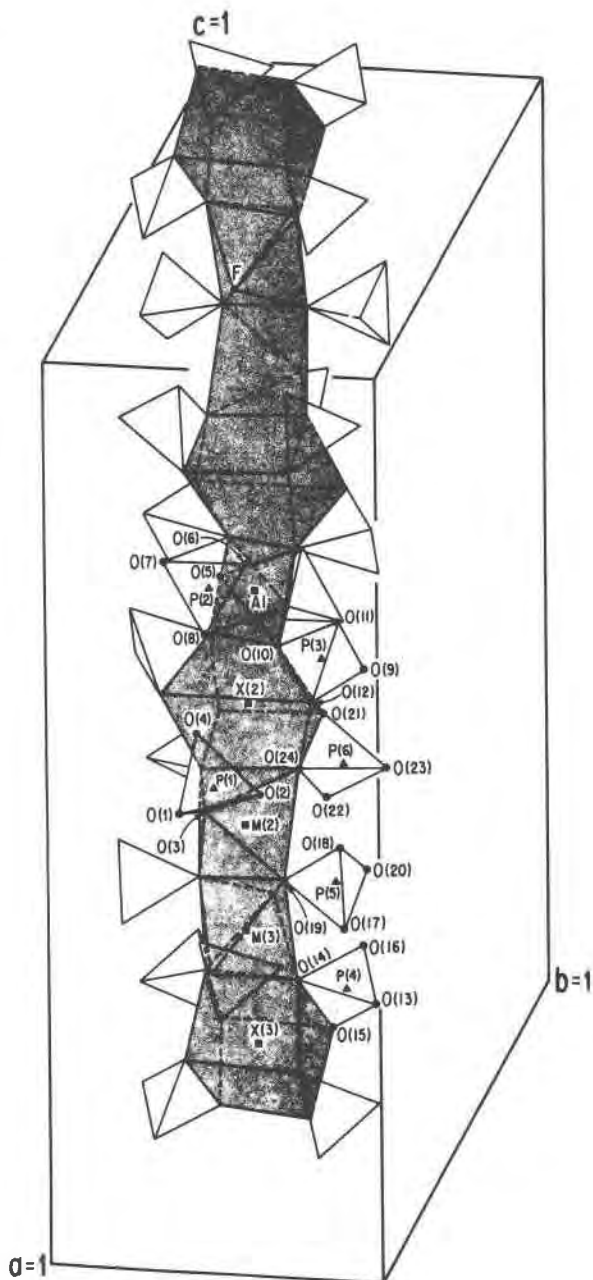
Fig. 4. Rod I in arrojadite (NM) drawn as a Penfield projection (Moore, 1981). The larger polyhedra are stippled and the enveloping transparent (PO_4) tetrahedra are drawn in. Note the sequence cube–octahedron–square pyramid–cube–octahedron–square pyramid–octahedron–cube. The Al site is an inversion center.

Table 6. Arrojadite–dickinsonite series bond distances and angles[a]

M(1)

	NM	NP	BR
M(1)-O(4)	1.969(6)	1.973(10)	2.069(7)
M(1)-O(8)[6]	2.022(4)	2.052(6)	2.084(4)
M(1)-O(12)[7]	2.042(3)	2.051(6)	2.082(4)
M(1)-O(11)	2.054(3)	2.081(6)	2.132(4)
average	2.022	2.039	2.092

	NM		NP	BR	
†O(4)-O(8)[6]	2.712(7)	85.6(2)	2.721(8)	2.781(8)	84.1(2)
O(4)-O(11)	3.164(6)	103.7(2)	3.159(10)	3.125(8)	96.1(2)
O(11)-O(12)[7]	3.259(5)	105.4(1)	3.294(7)	3.379(6)	106.2(2)
O(8)[6]-O(12)[7]	3.267(5)	123.0(2)	3.321(7)	3.280(6)	123.9(2)
O(4)-O(12)[7]	3.294(6)	110.4(2)	3.325(9)	3.379(9)	109.0(3)
O(8)[6]-O(11)	3.598(5)	123.9(2)	3.692(7)	3.774(6)	127.0(2)
average	3.216	108.7	3.252	3.285	107.7

M(2)

	NM	NP	BR
M(2)-O(19)	2.074(4)	2.080(6)	2.116(4)
M(2)-O(3)	2.077(12)	2.115(10)	2.095(6)
M(2)-O(20)[7]	2.113(4)	2.109(6)	2.134(4)
M(2)-O(24)[7]	2.117(4)	2.131(6)	2.177(4)
M(2)-O(23)	2.120(3)	2.120(5)	2.145(4)
average	2.100	2.111	2.133

|	NM		NP	BR	
*O(19)-O(23)	2.704(5)	80.3(2)	2.697(6)	2.738(6)	79.9(2)
O(3)-O(20)[7]	2.828(12)	84.9(3)	2.790(8)	2.819(7)	83.6(2)
†O(3)-O(23)	2.899(12)	87.4(3)	2.997(8)	3.032(7)	91.3(2)
O(20)[7]-O(23)	2.975(6)	89.3(2)	2.975(6)	3.025(6)	80.0(2)
O(19)-O(24)[7]	3.064(6)	93.9(2)	3.086(7)	3.131(6)	93.6(2)
†O(20)[7]-O(24)[7]	3.114(6)	94.8(2)	3.103(7)	3.134(6)	93.3(2)
O(3)-O(24)[7]	3.267(13)	102.3(4)	3.266(8)	3.289(7)	100.7(2)
O(3)-O(19)	3.284(13)	104.6(4)	3.434(8)	3.493(8)	112.1(3)
average	3.017	92.2	3.044	3.082	93.1

M(3)

	NM	NP	BR
M(3)-O(14)	2.036(3)	2.040(5)	2.065(4)
M(3)-O(23)	2.046(3)	2.059(6)	2.091(4)
M(3)-F	2.062(6)	2.076(6)	2.118(4)
M(3)-O(1)[5]	2.163(3)	2.186(6)	2.259(4)
M(3)-O(9)	2.164(3)	2.165(6)	2.212(4)
M(3)-O(19)	2.164(4)	2.152(6)	2.188(4)
average	2.106	2.113	2.156

	NM		NP	BR	
*O(19)-O(23)	2.704(5)	79.9(1)	2.697(6)	2.738(6)	79.5(2)
*O(1)[5]-O(9)	2.782(5)	80.0(1)	2.789(7)	2.836(5)	78.7(1)
F-O(23)	2.822(5)	86.8(2)	2.812(7)	2.885(6)	86.5(2)
O(1)[5]-O(14)	2.905(5)	87.5(2)	2.940(7)	3.004(5)	87.9(2)
F-O(19)	2.930(6)	87.8(2)	2.889(8)	2.971(6)	87.2(2)
†O(9)-O(14)	2.964(5)	89.7(1)	2.983(6)	2.998(6)	88.9(2)
F-O(9)	2.980(5)	89.7(2)	3.009(6)	3.049(6)	89.5(2)
†O(1)[5]-O(23)	3.013(6)	91.4(2)	3.063(6)	3.152(6)	92.8(2)
F-O(14)	3.028(5)	95.3(2)	3.032(6)	3.056(6)	93.8(2)
O(9)-O(23)	3.107(5)	95.1(1)	3.110(6)	3.198(6)	96.0(2)
O(14)-O(19)	3.109(5)	95.5(1)	3.101(7)	3.152(6)	95.6(2)
O(1)[5]-O(19)	3.369(6)	102.3(2)	3.404(6)	3.513(6)	104.4(2)
average	2.976	90.1	2.986	3.046	90.1

M(4)

	NM	NP	BR
M(4)-O(24)[5]	2.065(4)	2.067(5)	2.127(4)
M(4)-O(1)	2.090(3)	2.099(6)	2.105(4)
M(4)-O(9)[5]	2.144(3)	2.139(6)	2.132(4)
M(4)-O(7)	2.150(3)	2.157(6)	2.193(4)
M(4)-O(5)	2.194(3)	2.204(5)	2.219(4)
M(4)-O(15)[1]	2.216(4)	2.194(5)	2.226(4)
average	2.143	2.143	2.167

	NM		NP	BR	
†O(5)-O(7)	2.420(4)	67.7(1)	2.418(7)	2.426(5)	66.7(1)
*O(1)-O(9)[5]	2.782(5)	82.1(1)	2.789(7)	2.836(5)	84.0(1)
O(5)-O(15)[1]	2.824(4)	79.6(1)	2.831(6)	2.868(6)	80.4(1)
†O(9)[5]-O(15)[1]	2.974(5)	86.0(1)	2.967(6)	2.990(6)	86.6(2)
O(9)[5]-O(21)[5]	2.980(5)	90.1(1)	2.955(7)	3.006(6)	89.8(2)
O(5)-O(21)[5]	2.988(5)	89.1(1)	3.016(6)	3.067(5)	89.8(2)
O(7)-O(21)[5]	3.009(5)	91.1(2)	3.030(6)	3.067(5)	90.4(2)
†O(7)-O(15)[1]	3.140(5)	92.0(1)	3.125(7)	3.188(6)	92.3(2)
O(1)-O(15)[1]	3.150(5)	94.0(1)	3.139(6)	3.184(6)	94.6(2)
†O(1)-O(21)[5]	3.153(5)	98.7(1)	3.132(6)	3.164(6)	96.7(2)
O(1)-O(7)	3.277(5)	101.2(1)	3.302(6)	3.294(6)	100.0(2)
O(5)-O(9)[5]	3.527(4)	108.8(1)	3.523	3.548(5)	109.2(2)
average	3.019	90.0	3.019	3.053	90.0

M(5)

	NM	NP	BR
M(5)-O(17)[5]	2.027(4)	2.008(5)	2.047(4)
M(5)-O(6)	2.104(3)	2.117(6)	2.130(4)
M(5)-O(2)	2.106(3)	2.123(6)	2.156(4)
M(5)-O(11)	2.143(4)	2.116(5)	2.106(4)
M(5)-O(14)[5]	2.220(3)	2.239(6)	2.241(4)
M(5)-O(13)[5]	2.288(3)	2.304(6)	2.318(4)
average	2.148	2.150	2.166

	NM		NP	BR	
‡O(13)[5]-O(14)[5]	2.428(4)	65.2(1)	2.423(6)	2.423(5)	64.2(1)
*O(2)-O(6)	2.707(5)	80.0(1)	2.709(6)	2.740(6)	79.5(2)
O(6)-O(17)[5]	2.900(5)	89.2(2)	2.926(6)	2.922(5)	88.7(2)
†O(11)-O(14)[5]	2.913(5)	83.7(1)	2.899(6)	2.915(5)	84.1(2)
O(2)-O(11)	2.935(4)	87.3(1)	2.925(7)	2.944(5)	84.4(2)
O(11)-O(13)[5]	2.985(5)	84.6(1)	2.982(6)	2.992(5)	85.0(1)
†O(13)[5]-O(17)[5]	3.023(5)	88.8(1)	3.033(7)	3.085(6)	89.7(2)
O(14)[5]-O(17)[5]	3.057(5)	92.0(1)	3.042(7)	3.072(6)	91.4(2)
O(6)-O(1)	3.110(5)	94.1(1)	3.087(7)	3.121(6)	94.9(2)
O(2)-O(17)[5]	3.146(5)	99.1(2)	3.129(6)	3.168(6)	97.8(2)
O(6)-O(13)[5]	3.482(5)	104.8(1)	3.505(7)	3.527(6)	104.8(1)
O(2)-O(14)[5]	3.538(5)	109.7(1)	3.583(7)	3.633(5)	111.4(1)
average	3.019	89.9	3.020	3.045	89.9

A1

	NM	NP	BR
2 A1-O(5)[1]	1.862(3)	1.859(6)	1.894(4)
2 A1-O(10)	1.895(3)	1.890(5)	1.936(4)
2 A1-O(13)	1.896(3)	1.892(5)	1.915(4)
average	1.884	1.880	1.915

	NM		NP	BR	
2 O(5)[1]-O(13)[4]	2.587(4)	87.0(1)	2.588(6)	2.609(5)	86.5(2)
2 O(5)[1]-O(10)[4]	2.615(4)	88.2(1)	2.600(6)	2.636(5)	87.0(2)
†2 O(10)-O(13)	2.652(4)	88.8(1)	2.653(6)	2.700(5)	89.1(2)
2 O(5)[1]-O(10)	2.697(4)	91.8(1)	2.701(6)	2.779(6)	93.0(2)
2 O(10)[4]-O(13)	2.709(5)	91.2(1)	2.694(5)	2.746(5)	91.0(2)
2 O(5)[1]-O(13)	2.725	93.0(1)	2.715(5)	2.776(5)	93.6(2)
average	2.664	90.0	2.659	2.708	90.0

[a]Estimated standard errors in parentheses refer to the last digit. The equivalent positions (referred to Table 2) are designated as superscripts and are (1) = ½+x, -y, z; (2) = x, ½+y, ½+z; (3) = ½+x, ½-y, ½+z; (4) = -x, -y, -z; (5) = ½-x, y, -z; (6) = -x, ½-y, ½-z; (7) = ½-x, ½+y, ½-z. ☆P-X shared edges. †M-X shared edges. *X-X shared edges. ‡P-M shared edges. *M-M shared edges.

The disordered X(7) distances for NP are: 2 X(7)-O(19) = 2.79(1), 2 X(7)-O(2) = 2.98(1), 2 X(7)-O(3) = 2.99(2), 2 X(7)-O(1) = 3.16(2), 2 X(7)-O(18) = 3.20(3), 2 X(7)-O(17) = 3.35(3) Å, average 3.08 Å.

wyllieite and $c/12 = 3.63$Å in fillowite. Since arrojadite's structural principle more closely resembles wyllieite, the repeats between successive cations in a rod are quite similar.

Summing up, we propose a range of M and X populations in arrojadite's cell. Since X(1) is shown to be half-occupied and since X(6) and X(7) have steric problems then $\sum(M + X) = 84$ including half-occupied M(1). Omitting X(6) when P(1x) = 0, there can be 80 cations. If the large X(4) and X(7) sites are empty there exist 76 cations. The range, then, is most likely $\sum(M + X) = 76$–84 larger cations in the cell. Moore and Ito (1979) found a range between 76.8

and 85.9 cations in the cell (other than P^{5+}) based on nine different analyses for the mineral from various localities. The order of cation omission beyond X(6) would appear to be X(7) ≈ X(4) > X(5) ≫ X(3), that is the largest X(7) and X(4) sites would be the first to "leak" in a progressive oxidation-leaching of the mineral.

The underlying core of the arrojadite structure is rod I which occurs at the centers of the hexagons. In arrojadites, rod I appears to be fully populated with cations in the sequence ···X(3)–M(3)–M(2)–X(2)–Al–X(2)–M(2)–M(3)···. Figure 4 features a Penfield projection of this rod including its circumjacent PO₄

Table 6. (Continued)

	M(6)				M(7)		
	NM	NP	BR		NM	NP	BR
M(6)-O(18)	2.043(4)	2.055(5)	2.095(4)	M(7)-O(22)	2.055(4)	2.068(7)	2.100(4)
M(6)-O(6)	2.151(3)	2.166(6)	2.216(4)	M(7)-O(7)	2.090(3)	2.115(7)	2.166(4)
M(6)-O(12)[7]	2.167(4)	2.210(5)	2.219(4)	M(7)-O(16)[7]	2.165(4)	2.184(5)	2.185(4)
M(6)-F[7]	2.247(3)	2.236(6)	2.239(4)	M(7)-O(20)[7]	2.179(4)	2.208(7)	2.259(4)
M(6)-O(2)	2.254(3)	2.285(6)	2.338(4)	M(7)-F[7]	2.255(3)	2.236(6)	2.239(4)
M(6)-O(24)[7]	2.376(5)	2.342(7)	2.303(4)	average	2.149	2.162	2.190
average	2.206	2.216	2.235				
				[M(7)-O(4x)	2.38(2)	2.512(5)	2.40(3)]

	NM		NP	BR			NM		NP	BR	
*O(2)-O(6)	2.707(5)	75.8(1)	2.709(6)	2.740(6)	73.9(1)	†O(16)[7]-O(20)[7]	2.908(5)	84.1(1)	2.945(7)	2.974(6)	84.0(2)
O(6)-F[7]	2.911(5)	82.9(1)	2.906(7)	2.926(6)	82.1(2)	†O(7)-O(16)[7]	2.961(5)	88.2(1)	3.007(6)	3.094(5)	90.6(2)
O(6)-O(12)[7]	2.954(5)	86.3(1)	2.966(6)	3.032(5)	86.3(2)	O(7)-F[7]	3.002(5)	87.3(1)	2.982(7)	2.991(5)	85.5(2)
O(2)-O(12)[7]	2.993(5)	85.2(1)	3.040(6)	3.098(6)	85.6(2)	O(16)[7]-F[7]	3.038(5)	86.8(1)	3.051(6)	3.035(6)	86.6(2)
O(2)-O(18)	2.996(5)	88.3(2)	3.018(7)	3.035(6)	86.2(2)	O(20)[7]-O(22)	3.051(6)	92.1(2)	3.015(8)	3.068(6)	89.4(2)
O(18)-O(24)[7]	3.076(6)	87.9(2)	3.046(7)	3.062(6)	88.1(2)	O(22)-F[7]	3.066(6)	90.6(2)	3.065(7)	3.134(6)	92.5(2)
O(6)-O(18)	3.109(5)	95.6(2)	3.174(7)	3.169(6)	94.6(2)	O(7)-O(22)	3.106(5)	97.1(2)	3.180(8)	3.203(6)	97.3(2)
O(12)[7]-F[7]	3.110(5)	89.6(1)	3.134(7)	3.073(6)	87.1(2)	O(20)[7]-F[7]	3.728(5)	114.4(1)	3.765(7)	3.861(6)	118.3(2)
O(12)[7]-O(24)[7]	3.182(6)	88.8(1)	3.169(8)	3.168(6)	89.0(2)	average	3.107	92.6	3.126	3.170	93.0
O(18)-F[7]	3.236(5)	97.8(2)	3.258(6)	3.361(6)	101.6(2)						
O(2)-O(24)[7]	3.362(6)	93.1(1)	3.342(8)	3.345(6)	92.3(1)	[O(4x)-O(20)[7]	2.69(3)	72.1(6)	2.790(8)	2.81(3)	74.1(7)]
O(24)[7]-F[7]	3.738(5)	107.9(1)	3.742(7)	3.746(6)	111.1(2)	[O(4x)-O(22)	3.06(3)	86.9(5)	3.137(8)	3.43(3)	99.2(6)]
average	3.114	89.9	3.125	3.146	89.8	[O(4x)-O(7)	3.07(3)	86.6(6)	3.173(7)	2.98(3)	81.2(7)]
						[O(4x)-O(16)[7]	3.39(2)	96.3(5)	3.526(7)	3.06(3)	83.5(6)]

For NP, substitute O(3) for O(4x)

	X(6)		
	NM	NP	BR
X(6)-O(8)[6]	2.110(13)	2.113(13)	2.194(8)
X(6)-O(11)[1]	2.245(15)	2.297(14)	2.356(9)
X(6)-O(12)[7]	2.379(15)	2.331(14)	2.351(9)
X(6)-O(2)	2.527(13)	2.551(14)	2.549(8)
X(6)-O(15)[1]	3.217(15)	3.281(14)	3.386(9)
X(6)-O(12)[1]	3.282(16)	3.223(15)	3.204(10)
X(6)-O(10)[7]	3.305(14)	3.264(14)	3.252(8)
X(6)-O(1)	3.356(15)	3.436(14)	3.487(9)
X(6)-O(4x)	3.462(27)	3.488(14)	2.991(28)
X(6)-O(16)[7]	3.604(15)	3.580(14)	3.631(9)
average	2.949	2.956	2.940
average (inner four)	2.315	2.323	2.363

	P(1x)		
	NM	NP	BR
P(1x)-O(4x)	1.508(26)	1.434(10)	1.528(28)
P(1x)-O(1)	1.518(6)	1.514(8)	1.487(5)
P(1x)-O(2)	1.585(6)	1.565(8)	1.562(5)
P(1x)-O(3x)	1.639(19)	1.614(22)	1.724(24)
average	1.562	1.532	1.575

	NM		NP	BR	
O(3x)-O(4x)	2.491(27)	104.6(11)	2.298(22)	2.780(35)	117.4(13)
O(1)-O(2)	2.509(5)	107.9(4)	2.514(6)	2.515(6)	111.1(3)
O(2)-O(3x)	2.528(19)	103.3(8)	2.583(21)	2.622(25)	105.8(9)
O(1)-O(4x)	2.548(26)	114.7(10)	2.501(9)	2.473(28)	110.2(11)
O(1)-O(3x)	2.592(20)	110.3(8)	2.536(25)	2.588(27)	107.2(10)
O(2)-O(4x)	2.615(26)	115.4(10)	2.535(7)	2.453(30)	105.1(11)
average	2.547	109.4		2.572	109.5

Table 6. (Continued)

P(1)

	NM	NP	BR
P(1)-O(3)	1.502(11)	1.482(10)	1.515(6)
P(1)-O(2)	1.520(3)	1.511(6)	1.510(4)
P(1)-O(4)	1.555(5)	1.573(10)	1.528(7)
P(1)-O(1)	1.559(3)	1.558(7)	1.571(4)
average	1.534	1.531	1.531

	NM		NP	BR	
O(2)-O(4)	2.466(6)	106.6(3)	2.463(8)	2.435(8)	106.5(4)
☆O(1)-O(3)	2.484(12)	108.5(5)	2.501(9)	2.506(7)	108.6(3)
O(3)-O(4)	2.489(13)	109.0(5)	2.405(10)	2.455(9)	107.6(4)
O(1)-O(2)	2.509(5)	109.1(2)	2.514(6)	2.515(6)	109.4(3)
O(2)-O(3)	2.517(12)	112.8(5)	2.535(7)	2.528(7)	113.4(3)
O(1)-O(4)	2.564(6)	110.8(3)	2.565(8)	2.561(8)	11.4(4)
average	2.505	109.5	2.497	2.500	109.5

P(2)

	NM	NP	BR
P(2)-O(6)	1.521(3)	1.525(6)	1.524(4)
P(2)-O(8)	1.531(4)	1.528(5)	1.530(4)
P(2)-O(7)	1.552(3)	1.542(6)	1.546(4)
P(2)-O(5)	1.558(3)	1.557(6)	1.561(4)
average	1.541	1.538	1.540

	NM		NP	BR	
‡O(5)-O(7)	2.420(4)	102.2(2)	2.418(7)	2.426(5)	102.7(2)
☆O(7)-O(8)	2.502(5)	108.5(2)	2.490(6)	2.493(6)	108.3(2)
O(5)-O(6)	2.506(4)	109.0(2)	2.506(7)	2.508(5)	108.8(2)
O(6)-O(8)	2.528(5)	111.9(2)	2.527(6)	2.525(6)	111.5(2)
O(6)-O(7)	2.557(4)	112.6(2)	2.558(6)	112.8(2)	112.8(2)
O(5)-O(8)	2.564(5)	112.3(2)	2.555(6)	2.569(5)	112.5(2)
average	2.513	109.4	2.509	2.513	109.4

P(3)

	NM	NP	BR
P(3)-O(10)	1.530(3)	1.530(5)	1.529(4)
P(3)-O(9)	1.531(3)	1.539(6)	1.541(4)
P(3)-O(12)	1.547(3)	1.543(5)	1.552(4)
P(3)-O(11)	1.548(3)	1.545(6)	1.538(4)
average	1.539	1.539	1.540

	NM		NP	BR	
O(11)-O(12)	2.478(5)	106.4(2)	2.469(6)	2.471(5)	106.2(2)
☆O(10)-O(12)	2.488(4)	107.9(2)	2.490(6)	2.508(6)	109.0(2)
☆O(9)-O(11)	2.507(4)	109.1(2)	2.511(7)	2.508(5)	109.1(2)
O(9)-O(10)	2.515(4)	110.5(2)	2.518(6)	2.507(6)	109.5(2)
O(9)-O(12)	2.540(5)	111.2(2)	2.544(7)	2.553(6)	111.3(2)
O(10)-O(11)	2.546(4)	111.6(2)	2.545(6)	2.539(5)	111.8(2)
average	2.512	109.4	2.513	2.514	109.5

P(4)

	NM	NP	BR
P(4)-O(15)	1.529(3)	1.532(3)	1.524(4)
P(4)-O(16)	1.529(4)	1.524(5)	1.529(4)
P(4)-O(14)	1.548(3)	1.541(6)	1.547(4)
P(4)-O(13)	1.561(3)	1.556(5)	1.560(4)
average	1.542	1.538	1.540

	NM		NP	BR	
‡O(13)-O(14)	2.428(4)	102.7(2)	2.423(6)	2.423(5)	102.5(2)
☆O(15)-O(16)	2.496(5)	109.4(2)	2.489(6)	2.476(6)	108.4(3)
☆O(13)-O(16)	2.529(4)	109.9(2)	2.521(6)	2.536(5)	110.4(2)
☆O(14)-O(15)	2.538(4)	111.2(2)	2.532(7)	2.529(6)	110.9(2)
O(14)-O(16)	2.547(5)	111.8(2)	2.544(6)	2.553(6)	112.2(2)
O(13)-O(15)	2.559(4)	111.8(2)	2.560(7)	2.565(6)	112.5(2)
average	2.516	109.5	2.521	2.514	109.5

P(5)

	NM	NP	BR
P(5)-O(18)	1.518(3)	1.522(6)	1.522(4)
P(5)-O(17)	1.523(4)	1.528(6)	1.532(4)
P(5)-O(19)	1.544(4)	1.551(6)	1.544(4)
P(5)-O(20)	1.555(4)	1.546(7)	1.555(4)
average	1.535	1.537	1.538

	NM		NP	BR	
☆O(17)-O(18)	2.462(5)	108.1(2)	2.481(6)	2.488(6)	109.1(2)
☆O(17)-O(20)	2.491(5)	108.1(2)	2.490(7)	2.506(6)	108.5(2)
O(19)-O(20)	2.515(5)	108.5(2)	2.503(7)	2.509(6)	108.1(3)
O(18)-O(20)	2.518(5)	110.1(2)	2.510(8)	2.532(6)	110.8(2)
O(17)-O(19)	2.521(5)	110.5(2)	2.528(7)	2.515(6)	109.7(2)
O(18)-O(19)	2.531(5)	111.5(2)	2.540(7)	2.521(6)	110.6(3)
average	2.506	109.5	2.509	2.512	109.5

P(6)

	NM	NP	BR
P(6)-O(22)	1.537(4)	1.517(7)	1.528(4)
P(6)-O(23)	1.540(3)	1.537(6)	1.537(4)
P(6)-O(21)	1.542(4)	1.527(6)	1.532(4)
P(6)-O(24)	1.558(4)	1.564(8)	1.556(4)
average	1.544	1.536	1.538

	NM		NP	BR	
☆O(21)-O(22)	2.505(5)	108.9(3)	2.494(7)	2.499(6)	109.5(3)
☆O(21)-O(23)	2.510(5)	109.1(2)	2.506(6)	2.501(6)	109.2(2)
O(23)-O(24)	2.519(5)	108.8(2)	2.511(7)	2.514(6)	108.7(2)
☆O(21)-O(24)	2.527(6)	109.2(2)	2.522(7)	2.526(6)	109.8(3)
O(22)-O(24)	2.527(7)	109.5(3)	2.502(9)	2.511(7)	109.0(3)
☆O(22)-O(23)	2.541(5)	111.3(2)	2.515(8)	2.520(6)	110.6(3)
average	2.521	109.5	2.508	2.512	109.5

Continued

tetrahedra. Unlike fillowite, where face-sharing between polyhedra in its rod I is prevalent, in arrojadite only edge-sharing occurs. The sequence is ···cube–octahedron–square pyramid–cube–octahedron–cube–square pyramid–octahedron···. Opposing edges are shared in the chain. As mentioned before, rod VI

Table 6. (Continued)

X(1)

	NM	NP	BR
X(1)-O(8)[6]	2.240(5)	2.223(7)	2.279(5)
X(1)-O(16)[7]	2.247(4)	2.204(8)	2.239(5)
X(1)-O(15)[1]	2.310(4)	2.296(7)	2.324(5)
X(1)-O(4)	2.373(6)	2.354(10)	2.399(7)
X(1)-O(8)	2.483(5)	2.460(7)	2.506(5)
X(1)-O(16)[1]	2.596(4)	2.560(7)	2.595(5)
X(1)-O(7)	2.825(5)	2.824(8)	2.921(5)
X(1)-O(15)[6]	2.833(4)	2.883(8)	2.869(5)
average	2.489	2.476	2.516

	NM		BR	
☆2 O(15)[1]-O(16)[1]	2.496(5)	60.8(1)	2.476(6)	60.2(1)
☆1 O(7)-O(8)	2.502(5)	55.8(1)	2.493(6)	54.0(1)
†1 O(4)-O(8)[6]	2.712(7)	72.0(2)	2.781(8)	72.9(2)
1 O(4)-O(16)[7]	2.800(6)	74.6(2)	2.913(8)	77.7(2)
1 O(4)-O(15)[1]	2.805(7)	73.6(2)	2.800(9)	72.7(2)
†1 O(7)-O(16)[7]	2.961(5)	70.4(1)	3.094(5)	72.3(1)
†1 O(7)-O(15)[1]	3.140(5)	74.7(1)	3.188(6)	73.9(1)
1 O(4)-O(7)	3.141(6)	73.8(2)	3.285(8)	75.6(2)
2 O(8)-O(16)[7]	3.224(5)	85.8(1)	3.250(6)	86.3(2)
2 O(8)-O(15)[7]	3.385(5)	78.8(1)	3.488(6)	80.6(5)
2 O(8)-O(16)[1]	3.425(5)	84.8(1)	3.425(6)	84.3(2)
2 O(8)-O(15)[1]	3.498(5)	93.7(1)	3.466(6)	91.6(2)
average	3.088	76.6	3.104	76.8
[1 O(15)[6]-O(16)[1]	>3.75	103.0(2)	>3.75	103.0(1)]

X(2)

	NM	NP	BR
X(2)-O(10)	2.319(4)	2.338(7)	2.350(5)
X(2)-O(13)	2.336(4)	2.314(7)	2.344(5)
X(2)-O(24)	2.395(5)	2.416(8)	2.446(5)
X(2)-O(20)	2.420(4)	2.403(7)	2.404(5)
X(2)-O(21)	2.574(6)	2.531(9)	2.520(6)
X(2)-O(17)	2.675(6)	2.629(9)	2.685(6)
X(2)-O(16)	2.712(5)	2.802(8)	2.859(6)
average	2.490	2.490	2.515
[X(2)-O(12)	3.464(5)	3.545(6)	3.608(6)]

	NM		BR	
☆ O(17)-O(20)	2.491(5)	58.3(1)	2.506(6)	58.7(1)
☆ O(21)-O(24)	2.527(6)	61.0(2)	2.526(6)	61.1(2)
☆ O(13)-O(16)	2.529(4)	59.6(1)	2.536(5)	57.3(1)
† O(10)-O(13)	2.652(4)	69.5(1)	2.700(5)	70.3(2)
† O(16)-O(20)	2.908(5)	68.8(1)	2.974(6)	68.2(2)
† O(13)-O(17)	3.023(5)	73.9(1)	3.085(6)	75.3(2)
† O(20)-O(24)	3.114(6)	80.6(2)	3.134(6)	80.5(2)
★ O(17)-O(21)	3.315(5)	78.3(2)	3.496(7)	84.3(2)
O(10)-O(21)	3.424(5)	88.7(2)	3.473(6)	90.9(2)
average	2.887	71.0	2.937	71.8
☆[O(10)-O(12)	2.488(4)		2.508(6)]	
[O(12)-O(24)	3.182(6)		3.168(6)]	
[O(12)-O(16)	>3.75		>3.75	]

X(3)

	NM	NP	BR
2 X(3)-O(14)	2.349(3)	2.351(5)	2.367(4)
2 X(3)-O(15)	2.515(4)	2.528(6)	2.571(4)
2 X(3)-O(9)	2.599(4)	2.603(5)	2.581(4)
2 X(3)-O(11)	2.761(3)	2.747(6)	2.778(4)
average	2.556	2.557	2.574

	NM		BR	
☆2 O(9)-O(11)	2.507(4)	55.7(1)	2.508(5)	55.7(1)
☆2 O(14)-O(15)	2.538(4)	62.8(1)	2.529(6)	61.4(1)
†2 O(11)[4]-O(14)	2.913(5)	69.0(1)	2.915(5)	68.5(1)
†2 O(9)-O(14)	2.964(5)	73.4(1)	2.998(6)	74.5(1)
†2 O(9)-O(15)[5]	2.974(5)	71.1(1)	2.990(6)	71.0(1)
2 O(11)-O(15)	3.689(5)	88.6(1)	3.718(6)	88.0(1)
average	2.931	70.1	2.943	69.9

X(4)

	NM	NP	BR
2 X(4)-O(3)	2.486(13)	2.630(9)	2.756(9)
2 X(4)-O(23)	2.882(4)	2.958(7)	2.995(4)
2 X(4)-O(1)	2.888(4)	2.950(8)	3.018(7)
2 X(4)-O(22)	3.278(10)	3.191(8)	3.171(12)
2 X(4)-O(21)	3.356(8)	3.198(9)	3.120(11)
average	2.978	2.985	3.012

	NM		BR	
☆2 O(21)-O(22)	2.505(5)	44.4(2)	2.499(6)	46.8(2)
☆2 O(21)-O(23)	2.510(5)	46.7(1)	2.501(6)	48.3(1)
☆2 O(1)-O(3)	2.484(12)	54.4(3)	2.506(7)	51.2(2)
☆2 O(22)-O(23)	2.541(5)	48.2(1)	2.520(6)	48.1(1)
†2 O(3)-O(23)	2.899(12)	64.9(3)	3.032(7)	63.5(2)
†2 O(1)-O(23)[5]	3.013(6)	63.0(1)	3.152(6)	63.2(1)
†2 O(1)[5]-O(21)	3.153(5)	60.1(1)	3.164(6)	62.0(1)
2 O(3)-O(22)	3.136(12)	64.2(3)	3.184(8)	64.5(2)
2 O(21)[5]-O(22)	>4.000	77.6(3)	>4.000	88.9(4)
average	>2.916	58.2	>2.951	59.6

X(5)

	NM	NP	BR
2 X(5)-O(18)	2.653(4)	2.728(7)	2.811(5)
2 X(5)-O(22)	2.791(5)	2.885(9)	2.917(5)
2 X(5)-O(17)	2.838(4)	2.906(7)	2.974(5)
2 X(5)-O(21)	3.006(4)	3.024(7)	3.009(5)
average	2.822	2.886	2.928

	NM		BR	
☆2 O(17)-O(18)	2.462(5)	53.2(1)	2.488(6)	50.8(1)
☆2 O(21)-O(22)	2.505(5)	51.0(1)	2.499(6)	49.9(1)
2 O(18)-O(22)	3.242(6)	73.1(1)	3.384(7)	72.4(1)
★2 O(17)-O(21)	3.315(5)	69.0(1)	3.496(7)	71.5(1)
2 O(17)[5]-O(18)	3.593(6)	81.7(1)	3.637(6)	77.8(2)
2 O(21)[5]-O(22)	>4.000	91.5(2)	>4.000	96.1(2)
average	>3.520	69.9	>3.584	69.8

Table 6a. Rank of edge-sharing polyhedral distances and polyhedral types[a]

M(1)		X(1)	
†O(4)-O(8)[(6)]	1	☆O(15)[(1)]-O(16)[(1)]	1
		☆O(7)-O(8)	2
M(2)		†O(4)-O(8)[(6)]	3
*O(19)-O(23)	1	†O(7)-O(16)[(7)]	6
†O(3)-O(23)	3	†O(7)-O(15)[(1)]	7
†O(20)[(7)]-O(24)[(7)]	6		
		X(2)	
M(3)		☆O(17)-O(20)	1
*O(19)-O(23)	1	☆O(21)-O(24)	2
*O(1)[(5)]-O(9)	2	☆O(13)-O(16)	3
†O(9)-O(14)	6	†O(10)-O(13)	4
†O(1)[(5)]-O(23)	8	†O(16)-O(20)	5
		†O(13)-O(17)	6
M(4)		†O(20)-O(24)	7
‡O(5)-O(7)	1	*O(17)-O(21)	8
*O(1)-O(9)[(5)]	2		
†O(9)[(5)]-O(15)[(1)]	4	**X(3)**	
†O(7)-O(15)[(1)]	8	☆O(9)-O(11)	1
†O(1)-O(21)[( )]	10	☆O(14)-O(15)	2
		†O(11)[(4)]-O(14)	3
M(5)		†O(9)-O(14)	4
‡O(13)[(5)]-O(14)[(5)]	1	†O(9)-O(15)[(5)]	5
*O(2)-O(6)	2		
†O(11)-O(14)[(5)]	4	**X(4)**	
†O(13)[(5)]-O(17)[(5)]	7	☆O(21)-O(22)	1
		☆O(21)-O(23)	2
M(6)		☆O(1)-O(3)	3
*O(2)-O(6)	1	☆O(22)-O(23)	4
		†O(3)-O(23)	5
M(7)		†O(1)-O(23)[(5)]	6
†O(16)[(7)]-O(20)[(7)]	1	†O(1)[(5)]-O(21)	7
†O(7)-O(16)[(7)]	2		
		X(5)	
Al		☆O(17)-O(18)	1
		☆O(21)-O(22)	2
†O(10)-O(13)	3	★O(17)-O(21)	4

[a] Listed under the polyhedron, are shared edges in Table 6. The type of shared edge appears first (see footnote in Table 6) and the shared edge is followed by the rank or the sequence in the edge distance list.

is empty and rod II includes the disordered $X(1) = Ca^{2+}$. These rods are situated in the centers of the rhombuses in the net in Figure 2. Rods III, IV and V also involve P^{5+} cations and, like the fillowite study, their Penfield projections are not featured. Rod III involves the disordered cation X(6), and the large 10-coordinate X(4) and X(7) sites which appear to be

partly occupied. A sequence in rod III would be $\cdots X(5)-P(2)-M(1)-P(1)-_{X(4)}^{[X(7)]}-P(1)-M(1)-P(2)\ \cdots$. Rod IV has the sequence $\cdots P(3)-M(6)-P(5)-M(5)-P(3)-M(6)-P(5)-M(5)\cdots$. Rod V has the sequence $\cdots M(4)-P(6)-M(7)-P(4)-M(4)-P(6)-M(7)-P(4)\cdots$.

Bond distances and angles

Bond distances and angles for the Nancy Mine arrojadite (NM), Nickel Plate arrojadite (NP) and Branchville dickinsonite (BR) are presented in Table 6. Owing to inferior data, X(7) is not included in the discussion. Since data for three independent crystals have been obtained and since the asymmetric unit is so complex, only a portion of the information is presented in some cases. For example, data for NM, NP and BR are given for M(1) through M(7) and Al, and P(1) through P(6); but for the X polyhedra only the O–O′ distances are given for NM and BR; and just NP for X(7). Five types of shared edges can be discerned: an edge shared between P and M symbolized by ‡, an edge between P and X (☆), an edge between M and M′ (*), an edge between M and X (†), and an edge between X and X′ (★). We believe the order of increasing O–O′ distances to be ‡ < ☆ < * < † < ★, following the order of increasing polyhedral size based on ionic radius, bond strength and cation-cation repulsion across the shared edge. That is to say, the progression of increasing distances follows the expected size of the smaller of the two polyhedra in an edge-sharing pair, and the bond strength associated with that polyhedron. Thus, with the relatively rigid (PO₄) tetrahedron we would expect distances involving (PO₄) to appear on the top of the list in Table 6 since these distances were tabulated according to increasing size for that polyhedron.

This is quite clearly the case in Table 6. Distances associated with (PO₄) always appear on the top of the list for other polyhedra. Next appear the distances involving M–M′. Distances involving M–X and X–X′ appear next, but often these occur after a gap in cases where some O–O′ distances involving no shared edges occur with shorter distances. This is easily understandable since X are usually polyhedra of high order (>6) and of low cation charge (Na^{1+} and K^{1+} for example). To assist the reader in identifying the shared edge distances in the various polyhedra and the sequence of these distances according to increasing polyhedral size in Table 6, the polyhedra are listed in Table 6a. Table 7 lists the next larger distance in the crystal which is not listed in Table 6. For the fourteen distinct larger cation–oxygen polyhedra excluding X(7), ten of the bonds are underlined since

these are cation–anion bonds not included and are therefore potential coordinating anions. However, a substantial gap exists between that distance and the distance in the preceding column except for M(7)–O(3) and X(2)–O(5). These are precisely the cations where an ambiguity in coordination number is indicated. For the bond length–bond strength calculations, the inner coordination sphere was used. With respect to the bond length-bond strength tabulations in Table 9[3], of the 93 individual entries, 60 show the expected correlation between individual distance deviation from the polyhedral mean and electrostatic bond strength sum deviations from neutrality. Those that do not are compensated for by deviations with opposing sign in the same row.

Perhaps the most interesting case is the $M(1)O_4$ distorted tetrahedron. As mentioned above, steric hindrance involving X(6) should reduce the M(1) site occupancy by the amount equivalent to the X(6) population. The next nearest contact with M(1) is X(1) and the close approach between these cations is due to the O(4)–O(8)[6] shared edge between these two polyhedra. There is an additional problem with the M(1) site, namely, not only does the X(6) population influence M(1), but the unusual [4]M(1)–O 2.02Å average distance in NM arrojadite suggested that the Li^{1+} reported in analyses of arrojadites may be ordered in this site (an average distance of [4]Li^{1+}–O 1.98Å is reported by MacGillavry and Rieck, 1968). Therefore, we took the refined site population for M(1), which was based solely on a scattering curve for Fe^{2+}, and recalculated the Li^{1+} cell content assuming that the site was fully occupied. This yielded an upper limit of 3.30 Li^{1+} in the cell for NM arrojadite and 4.74 Li^{1+} for BR dickinsonite. For the NP arrojadite, the low Li^{1+} content (0.5 atom) was placed in the site. Although the calculated value for NM arrojadite is in fair agreement with Table 8, the calculated value for BR dickinsonite is much too high. Therefore, we had an atomic absorption analysis done on a Branchville dickinsonite (Brush and Data, Yale No. 3090 specimen), which yielded 0.448 wt.% Li_2O or about 2.50 atoms of Li in the cell. We thank Dr. Andrew Davis for this determination.

The alternative to having M(1) fully occupied by Fe + Li is to assume that this site is partially vacant and that its occupancy complements the occupancy at X(6), since the X(6)–M(1) 0.66Å distance in NM

Table 8. Arrojadite–dickinsonite selected chemical analyses and interpretation

	1	2	3	4	5	6
P_2O_5	39.54	40.93	45.34	40.00	40.1	39.5
Fe_2O_3	---	---	---	nil	nil	---
Al_2O_3	2.37	---	10.86	2.66	2.33	2.0
FeO	46.70	---	30.60	28.22	34.9	13.3
MnO	---	47.72	---	15.78	7.76	32.0
MgO	---	---	---	1.04	3.37	nil
CaO	2.60	5.39	---	2.46	3.65	2.3
Li_2O	---	---	---	0.09	0.52	0.45
Na_2O	5.76	5.96	13.20	6.40	5.36	7.8
K_2O	2.19	---	---	1.74	1.43	1.1
H_2O	0.84	---	---	0.91	0.14	1.65
F	---	---	---	0.80	n.d.	---
Insol	---	---	---	0.11	---	---
Rem	---	---	---	---	0.68	---
Total	100.00	100.00	100.00	100.21	100.29	100.1
O = F	---	---	---	-0.34	---	---

[1]Theoretical composition, $KNa_4CaFe^{2+}_{14}Al(OH)_2(PO_4)_{12}$, of end member arrojadite.

[2]Theoretical composition, $Na_2CaMn^{2+}_7(PO_4)_6$, end member fillowite.

[3]Theoretical composition, $Na_2Fe_2Al(PO_4)_3$, end member ferro-wyllieite.

[4]Arrojadite from Nickel Plate pegmatite, South Dakota. Analysis by Lindberg (1950).

[5]Arrojadite from Nancy Mine, New Hampshire. Ito analysis in Moore and Ito (1979). The *n.d.* means not determined. *Rem* includes PbO 0.37, ZnO 0.24, BaO 0.02 and SrO 0.05.

[6]Dickinsonite from Branchville, Connecticut. Irving analysis in Moore and Ito (1979) by electron probe. Li_2O was determined by Dr. Andrew Davis employing atomic absorption spectrometry and H_2O was reported by Wells in Brush and Dana (1890).

arrojadite suggests a coupled relationship between these sites. The possible Li^{1+} populations in M(1) are given as a footnote in Table 7. It is difficult to decide which model is better, but the one which affords the fewest contradictions appears to be the complementary relationship between M(1) and X(6).

One of the continuing problems has been the suspected dimorphism between dickinsonite and fillowite. Despite their noteworthy similarity in chemical composition (compare columns 1 and 3 in Table 8), the structures are based on different principles. As discussed by Moore (1981), fillowite is based on the regular hexagonal rod-packing whose Schläfli symbol is {6³}, while dickinsonite is based on a rod-packing over a net which is neither regular nor semiregular, that is, the net composed of nodes {6 · 3 · 6 · 3} and {6 · 6 · 3 · 3}. Fillowite is related to a large family of glaserite-derived structures, while dickinsonite and wyllieite seem to stand alone in a different family of distinct but remotely related struc-

³ To obtain copy of Table 9, order Document AM-81-172. See Footnote one for details.

Table 10. Arrojadite–dickinsonite: calculated and observed powder diffraction data[†]

I(calc)	d(calc)	hkℓ	I(obs)	d(obs)	I(calc)	d(calc)	hkℓ	I(obs)	d(obs)
11	12.010	200	10	12.105	51	2.737	622	70	2.719
31	7.717	202	20	7.734	4	2.695	233	5	2.676
11	6.550	211	10	6.524	6	2.621	$\bar{6}$31	5	2.650
15	5.985	202	30	5.983	9	2.583	820	10	2.603
17	5.588	$\bar{4}$02	20	5.584	16	2.577	424	10	2.567
17	5.065	020	30	5.059	12	2.533	040	20	2.552
13	4.618	411	10	4.615	8	2.447	$\bar{8}$24	20	2.517
2	3.496	$\bar{6}$13	--	-----	7	2.440	$\bar{2}$26	10	2.429
3	3.486	520	10	3.475	5	2.410	$\bar{4}$26	20	2.413
16	3.443	611	30	3.430	2	2.361	$\bar{5}$26	5	2.390
8	3.355	413	10	3.365	1	2.334	440	5	2.342
4	3.305	031	20	3.334	2	2.302	813	10	2.313
4	3.275	422	5	3.288	1	2.290	$\bar{1}$17	--	-----
33	3.253	602	50	3.234	1	2.286	$\bar{8}$31	5	2.283
13	3.233	$\bar{2}$31	--	-----	4	2.278	$\bar{5}$36	--	-----
5	3.161	$\bar{6}$22	--	-----	1	2.244	017	--	-----
7	3.160	$\bar{7}$13	--	-----	4	2.240	540	--	-----
3	3.148	$\bar{1}$15	10	3.149	6	2.222	$\bar{6}$17	10	2.222
5	3.143	231	10	3.126	2	2.213	$\bar{7}$26	15	2.200
5	3.071	$\bar{4}$15	--	-----	2	2.170	10.20	--	-----
100	3.070	$\bar{4}$24	100	3.055	1	2.165	$\bar{2}$44	--	-----
18	2.875	$\bar{2}$33	--	-----	1	2.149	10.02	--	-----
8	2.863	$\bar{8}$13	--	-----	1	2.146	804	--	-----
8	2.858	033	20	2.854	1	2.140	326	--	-----
2	2.841	720	10	2.843	1	2.130	$\bar{7}$35	5	2.132
4	2.830	431	--	-----	1	2.117	$\bar{4}$44	--	-----
12	2.808	$\bar{6}$16	10	2.814	1	2.085	$\bar{4}$08	--	-----
10	2.794	$\bar{8}$04	20	2.781	1	2.046	426	--	-----
11	2.784	$\bar{2}$06	10	2.753	3	2.013	008	--	-----

[†]The calculated data are from the dickinsonite (BR) refined structure. The observed data are from Table 2, column II in Fisher (1965) based on Guinier camera, Co/Fe radiation and a Nickel Plate (NP) arrojadite sample. His intensity data are ×10.

tures. Fillowite has one rod which consists of a sequence of five face-sharing octahedra. No such region exists in the dickinsonite structure. The formulae of the two species may be compared, viz.:

fillowite Na_4 Ca_2 $Mn^{2+}_{14}(PO_4)_{12}$

dickinsonite Na_4 CaK $Mn^{2+}_{14}(PO_4)_{12} \cdot Al(OH)_2$.

Finally, with knowledge of the structure, a calculated powder pattern was obtained for the Branchville dickinsonite. Table 10 offers the prominent reflections to 2.00Å, and the calculated data are compared with the observed data of Fisher (1965) for a Nickel Plate arrojadite. The agreement is good, the major advantage being the correct choice of Miller indices for such a complex structure.

Table 11[4] is based on the list of eleven chemical analyses on arrojadite–dickinsonite presented by Moore and Ito (1979), but differs in possessing cell contents based on 200 anions, not 196 anions of the earlier study when the structure was unknown. This table partitions the cations into three categories: those cations believed to belong to the Al and M sites, the large cations of the X sites, and cell contents of P^{5+}. For the last, some totals exceeded 48 when the computation commenced with 200 anions and for these, the contents were computed based on $\sum P^{5+} = 48.0$.

If all M and Al sites were occupied, at most 60 M + Al cations would occur. Owing to the M(1)–X(6) couple, this number may be reduced to 56 M cations when X(6) is half-occupied. Table 11 shows that eight of the eleven analyses have more than 56 M + Al cations, but only four have more than 60 cations, three of them (2, 5, 8) barely over the theoretical limit. It is likely that a fairly large octahedral cation with respect to oxide coordination like Mn^{2+} may partition into the larger set of alkali and alkaline earth sites so that this group of smaller cations may represent a larger average than actually present in the Al and M(1) through M(7) positions.

Some solution involving $(OH)^-$ for O^{2-} or $(H_4O_4)^{4-}$ for $(PO_4)^{3-}$ may occur but this appears to be quite limited. The only flagrant deviation from quantitative $(PO_4)^{3-}$ occupancy is the material from Serra

---

[4] To obtain a copy of Table 11, order Document AM-81-173. See Footnote one for details.

Branca of Guimarães (1942). This material also was reported to have a high H_2O content. This material may be either of doubtful purity, extensively altered through hydrothermal reworking or even a different phase. Noteworthy in this light is the paucity of knowledge on arrojadite-dickinsonite alteration, the phase normally found in surprisingly unaltered and unleached form.

Acknowledgments

References

Araki, T. and Moore, P. B. (1981) Fillowite, $Na_2Ca(Mn,Fe)_7^{2+}$ $(PO_4)_6$: its crystal structure. American Mineralogist, 66, 827–842.

Britton, D. and Dunitz, J. D. (1973) A complete catalogue of polyhedra with eight or fewer vertices. Acta Crystallographica, A29, 362–371.

Brush, G. J. and Dana, E. S. (1878) On a new and remarkable mineral locality in Fairfield County, Connecticut; with a description of several new species occurring there. American Journal of Science, 16, 33–46.

Cromer, D. T. and Mann, J. B. (1968) X-ray scattering factors computed from numerical Hartree-Fock wave-functions. Acta Crystallographica, A24, 321–324.

Fisher, D. J. (1965) Dickinsonites, fillowite and alluaudites. American Mineralogist, 50, 1647–1669.

Guimarães, Dj. (1942) Arrojadita, um novo mineral do grupo da Wagnerita. Boletin Faculdad Filosofie Ciências Lettres XXX (São Paulo), Mineralogia No. 5, 4–15.

Headden, W. P. (1891) A phosphate near triphylite from the Black Hills. American Journal of Science, 41, 416–417.

Ibers, J. A. and Hamilton, W. C. (1974) International Tables for X-ray Crystallography, 4, The Kynoch Press, Birmingham, England, 99–100.

Krutik, V. M., Pushcharovskii, D. Yu, Pobedimskaya, E. A. and Belov, N. V. (1979) Crystal structure of arrojadite. Kristallografiya, 24, 743–750.

Lindberg, M. L. (1950) Arrojadite, hühnerkobelite and graftonite. American Mineralogist, 35, 59–76.

MacGillavry, C. H. and Rieck, G. D. (1962) International Tables for X-ray Crystallography, 3, The Kynoch Press, Birmingham, England, p. 258.

Main, P., Woolfson, M. M., Lessinger, L., Germain, S. and Declerq, J. P. (1977) MULTIN 74, a system of computer programs for the automatic solution of crystal structures. University of York (1974).

Mason, B. (1941) Minerals of the Varuträsk pegmatite. XXIII Some iron-manganese phosphate minerals and their alteration products, with special reference to material from Varuträsk. Geologiska Föreningens Förhandlingar, 63, 129–134.

Merlino, S., Mellini, M. and Zanazzi, P. F. (1981) The crystal structure of arrojadite. Acta Crystallographica, in press.

Moore, P. B. (1981) Complex crystal structures related to glaserite, $K_3Na(SO_4)_2$: evidence for very dense packings among oxysalts. Bulletin de la Société française de Minéralogie et de Cristallographie, in press.

Moore, P. B. and Ito, J. (1979) Alluaudites, wyllieites, arrojadites: crystal chemistry and nomenclature. Mineralogical Magazine, 43, 227–235.

Moore, P. B. and Molin-Case, J. A. (1974) Contribution to pegmatite phosphate giant crystal paragenesis: II. The crystal chemistry of wyllieite, $Na_2Fe_2^{2+}Al(PO_4)_3$, a primary phase. American Mineralogist, 59, 280–290.

Palache, C., Berman, H. and Frondel, C. (1960) The System of Mineralogy of Dana, 2 (7th Ed.), Wiley, New York, pp. 679–681; 717–720.

Quensel, P. (1937) Minerals of the Varuträsk pegmatite. I. The lithium-manganese phosphates. Geologiska Föreningens Förhandlingar, 59, 77–96.

Wolfe, C. W. (1941) The unit cell of dickinsonite. American Mineralogist, 26, 338–342.

Ziegler, V. (1914) The Minerals of the Black Hills. South Dakota School of Mines Bulletin No. 10 (Department of Geology and Mineralogy), 192–194.